

# CITY OF ALBUQUERQUE



March 5, 2018

Diane Hoelzer, P.E.  
Mark Goodwin & Associates  
PO Box 90606  
Albuquerque, NM, 87199

**RE: Juan Tabo Hills Estates  
Manhole 47 Drainage Report  
Stamp Date: 3/1/18  
Hydrology File- M21D018; DRB# 1005278**

Dear Ms. Hoelzer:

Based on the information provided in your submittal received 2/28/18, this submittal cannot be approved for Work Order by Hydrology.

PO Box 1293

Albuquerque

NM 87103

[www.cabq.gov](http://www.cabq.gov)

1. The proposal to re-align the inverts at Manhole 47 and maintain supercritical flow down the trunk to Tijeras Arroyo is unacceptable as the resulting hydraulic jump at the downstream junction box poses too great a hazard.
2. The proposed Energy Grade Line along the trunk under Sandia Sunset is too far above ground even for pressure manholes to be considered. Any unanticipated hydraulic jump along this trunk would be damaging to public and private property.
3. The excessive energy from the upstream storm drain will need to be dissipated at manhole 47. One option may be to lengthen manhole 47, creating a chamber long enough to force the R-2 flow regime as referenced in your report.

If you have any questions, you can contact me at 924-3695 or [dpeterson@cabq.gov](mailto:dpeterson@cabq.gov).

Sincerely,

A handwritten signature in black ink, appearing to read "Dana Peterson".

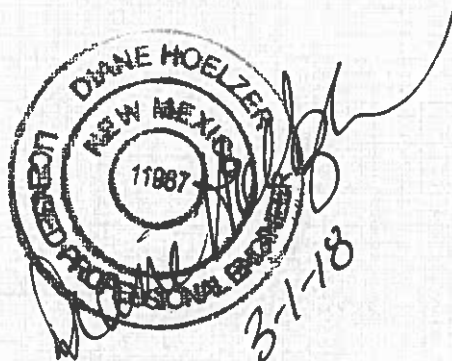
Dana Peterson, P.E.  
Senior Engineer, Planning Dept.  
Development Review Services

*Juan Tabo Estates*  
*(Residential Subdivision)*

*Drop Manhole 47*  
*Hydraulic Analysis*

*Prepared by*  
*Mark Goodwin & Associates, P.A.*

*March 2018*





# City of Albuquerque

Planning Department  
Development & Building Services Division

## DRAINAGE AND TRANSPORTATION INFORMATION SHEET (REV 09/2015)

Project Title: Juan Tabo Hills Estates	Building Permit #:	City Drainage #: M-21D018
DRB#: 1005278	EPC#:	Work Order#: 665888
Legal Description: Tract A Juan Tabo Hills West/Tract 1-A-1 Juan Tabo Hills Unit 2		
City Address: Juan Tabo and Tijeras Arroyo		
Engineering Firm: Mark Goodwin & Associates, PA		Contact: Diane Hoelzer, PE
Address: PO BOX 90606, Albuquerque, NM 87199		
Phone#: 505-828-2200 Fax#:		E-mail: diane@goodwinengineers.com
Owner: Eastland Development, Inc.		Contact: Rex Wilson
Address: PO BOX 9470, Albuquerque, NM 87119		
Phone#: 505-899-6768 Fax#:		E-mail: rwr2d2@aol.com
Architect:	Contact: _____	
Address:		
Phone#:	Fax#:	E-mail: _____
Other Contact: Aldrich Land Surveying	Contact: Tim Aldrich	
Address: PO BOX 30701, Albuquerque, NM 87190		
Phone#: 505-328-3988 Fax#:	E-mail: tim.aldrich@comcast.net	

Check all that Apply:

**DEPARTMENT:**

- HYDROLOGY/ DRAINAGE  
 TRAFFIC/ TRANSPORTATION  
 MS4/ EROSION & SEDIMENT CONTROL

**TYPE OF SUBMITTAL:**

- ENGINEER/ ARCHITECT CERTIFICATION  
  
 CONCEPTUAL G & D PLAN  
 GRADING PLAN  
 DRAINAGE MASTER PLAN  
 DRAINAGE REPORT  
 CLOMR/LOMR  
  
 TRAFFIC CIRCULATION LAYOUT (TCL)  
 TRAFFIC IMPACT STUDY (TIS)  
 EROSION & SEDIMENT CONTROL PLAN (ESC)  
 OTHER (SPECIFY) Hydraulic Analysis Manhole 47

**CHECK TYPE OF APPROVAL/ACCEPTANCE SOUGHT:**

- BUILDING PERMIT APPROVAL  
 CERTIFICATE OF OCCUPANCY  
  
 PRELIMINARY PLAT APPROVAL  
 SITE PLAN FOR SUB'D APPROVAL  
 SITE PLAN FOR BLDG. PERMIT APPROVAL  
 FINAL PLAT APPROVAL  
 SIA/ RELEASE OF FINANCIAL GUARANTEE  
 FOUNDATION PERMIT APPROVAL  
 GRADING PERMIT APPROVAL  
 SO-19 APPROVAL  
 PAVING PERMIT APPROVAL  
 GRADING/ PAD CERTIFICATION  
 WORK ORDER APPROVAL  
 CLOMR/LOMR  
  
 PRE-DESIGN MEETING  
 OTHER (SPECIFY) Construction CPN 665888 sheet 5R revised

IS THIS A RESUBMITTAL?:  Yes  No

DATE SUBMITTED: March 1, 2018 By: Diane Hoelzer, PE

COA STAFF:  ELECTRONIC SUBMITTAL RECEIVED:

Juan Tabo Hills Estates Storm Sewer Trunkline  
(CPN 665888)

**Hydraulic Analysis of the Drop Manhole 47**

**Purpose**

At the eastern boundary of Juan Tabo Hills Estates, there is a thirty foot drop in elevation between Juan Tabo Hills Unit 1 and 2 and this new development. There is an existing 84" RCP discharge pipe just south of Gallant Fox Road in the open space area that discharges from the upper JTH to the lower JTH Estates subdivision. At this location a 12.05 ft. drop manhole was designed to be constructed. The previous design Engineer had intended for this drop manhole to be used to dissipate energy and slow down velocities downstream. However, the actual hydraulics of this situation was not analyzed. During construction, one of the City stormwater maintenance Engineers expressed concern over both the structural and hydraulic functionality of this drop manhole.

As a follow up to his concerns, the 10' diameter manhole was structurally designed to handle the momentum forces associated with the 100 year storm discharges. The hydraulics of the drop manhole was also investigated, which is the purpose of this report.

**Introduction**

In steep terrains in urban area, drop manholes are sometimes used to dissipate energy. Drop manholes may lead to poor hydraulics if they are not designed properly to dissipate excess energy. Inadequately designed drop manholes can adversely affect upstream and downstream flow conditions.

According to the referenced paper, "the dominant hydraulic features of drop manholes depends on the flow regimes, characterized in terms of the dimensionless impact parameter."

Depending on what flow regime the drop structure is determined to be in, the relative pool height can also be calculated. The pool height is measured upward from the invert of the drop manhole.

For the particular condition at drop manhole 47, both of these values were calculated to determine if drop manhole would dissipate the excess energy from the upstream 84" storm pipe discharging from JTH Unit 1 and 2 developments in an adequate and safe manner, without affecting upstream or downstream flow conditions.

### Assumptions used in this analysis:

1. The referenced scientific paper is directly applicable to our situation.
2. The discharge values from the JTH Unit 1 and 2 as built drawings are accurate.
3. The pipe sizes and invert elevations in the as built JTH Unit 1 and 2 drawings are accurate.

### Calculations and Results

The Impact number is defined as:

$$I = ((2 \times s) / g)^{0.5} \times (V_{up}/D_m) \quad \text{where:}$$

s= drop height

g=gravity acceleration

V<sub>up</sub>=upstream pipe velocity

D<sub>m</sub>=diameter of drop manhole

$$\text{For our condition: } I = ((2 \times 12.05f) / 32.2f/s^2)^{0.5} \times (24.6 \text{ fps}/10f) = 2.128$$

According to Figure 5 our situation is in flow regime R3b. Flow regime R3b is "established by high approach flow Froude numbers with the water jet spreading radially over the manhole wall. A spiraling flow runs along the manhole wall interfering for high discharges ..."

According to Figure 5 this flow regime shows a relatively high energy loss in the manhole of approximately 0.87 percent.

"If the manhole operates under Regime 3, the drop manhole outflow is similar to orifice flow. Energy considerations lead to:

$$H_p/D_{out} = 0.6 + (7.3 - (D_m/D_{out}) \times (Q^*)^2)$$

$$\text{Where } Q^* = Q/(g \times D_{out}^5)^{0.5}$$

H<sub>p</sub> = pool height (in manhole)

D<sub>out</sub> = diameter of outfall pipe = 7.0 ft

D<sub>m</sub> = diameter of drop manhole = 10 ft

Q\* = non-dimensional discharge

Q = discharge value = 809 cfs

G = gravity acceleration = 32.2 f/s<sup>2</sup>

Results:

$$Q^* = 1.0997$$

$$H_p/D_{out} = 7.70$$

$$H_p = 53.9 \text{ ft (unacceptable, discharge above top of manhole).}$$

**Conclusion:**

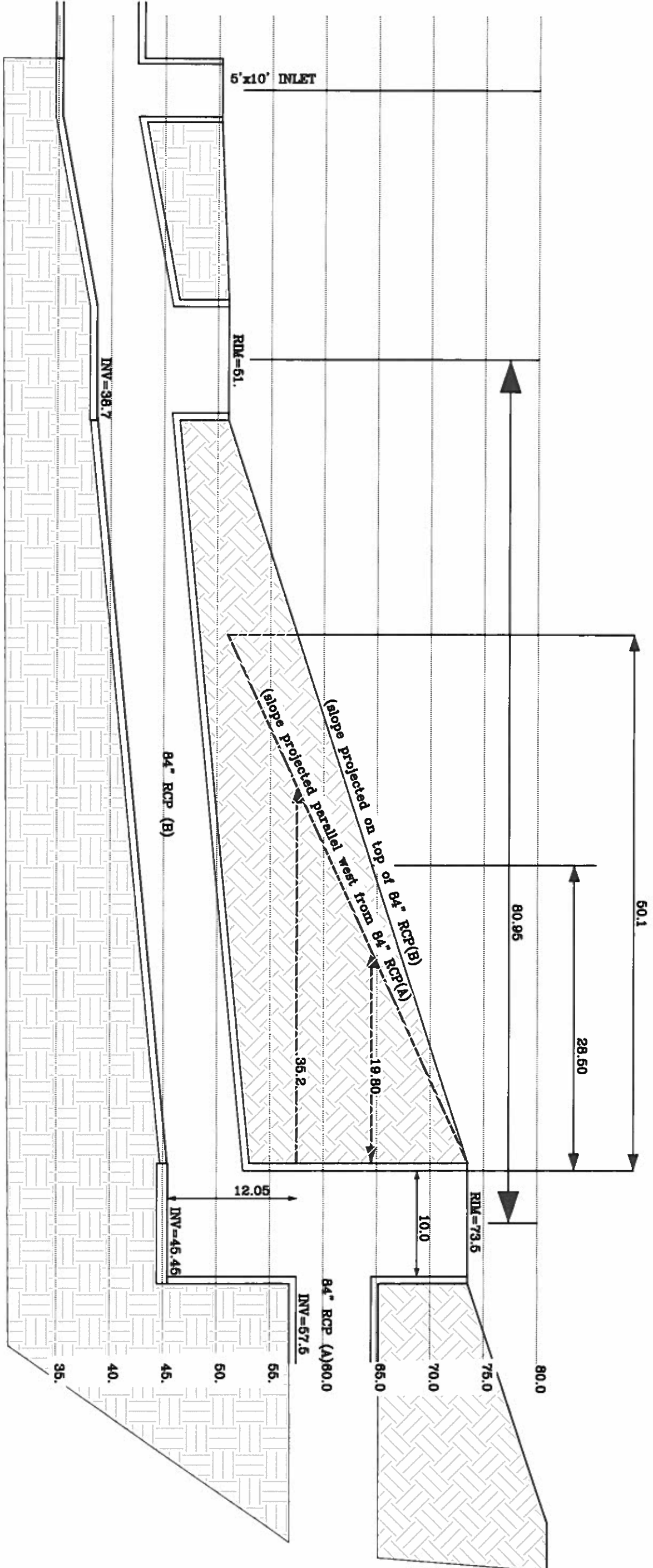
A drop manhole at this location cannot be designed in such a manner that will dissipate energy in a way that will not adversely affect the upstream and downstream flow regimes, and in this case the turbulence will over top the manhole 47 cover and possibly the downstream inlets.

An alternative design that was checked using the WSPGP storm model, was to connect manhole 47 invert directly to the invert of the downstream manhole 9 located at the toe of the sloped area in JTH Estates. This revision does increase the downstream velocities, but the HGL is well within the inside of the storm pipe and supercritical flow is maintained all the way to the junction box.

- Attachments:
- 1) Exhibit I – Existing Storm Drain Manhole 47 Design
  - 2) Exhibit II – Proposed Revised Storm Drain Manhole 47 Design
  - 3) Reference: Granata F., de Marinis G., Gargano R., Hager W.H. (2011). "Hydraulics of Circular Drop Manholes." Journal of Irrigation and Drainage Engineering 137(2): 102-111.

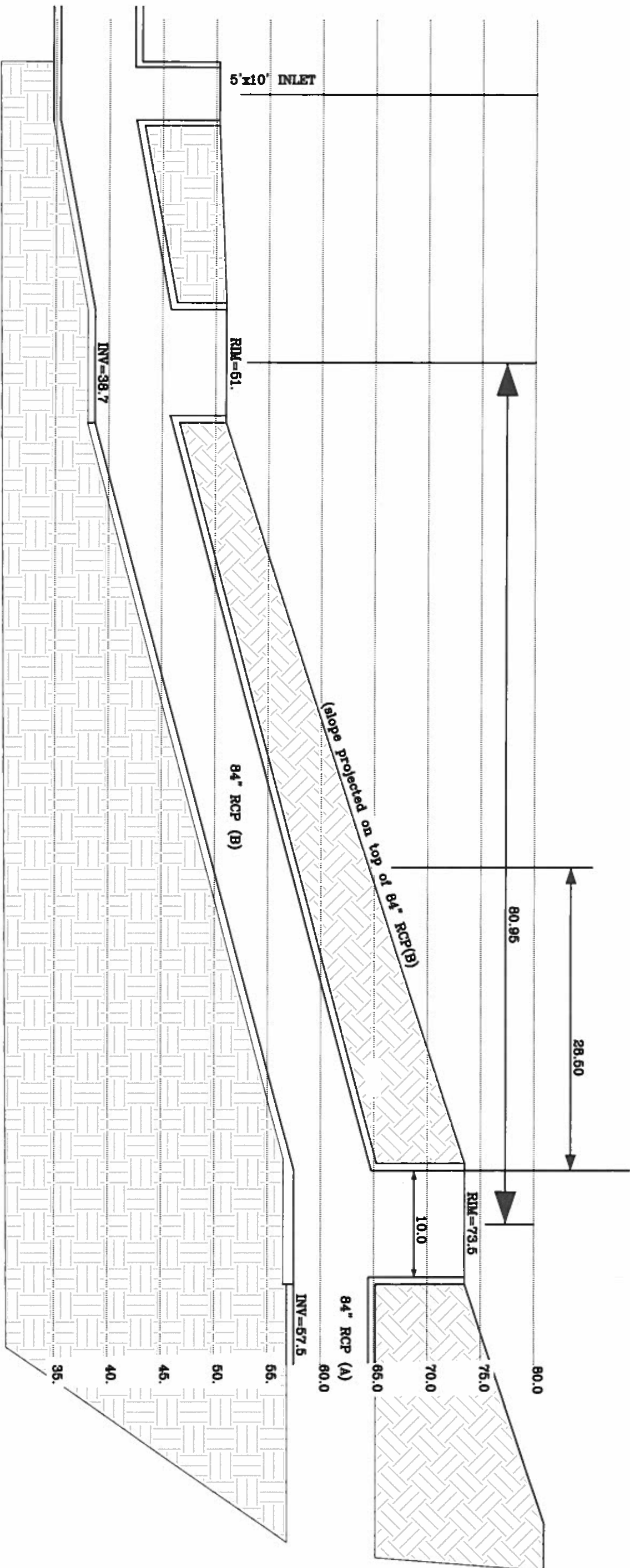
Diane Hoelzer, PE  
2-26-18





JUAN TABO HILLS ESTATES STORM DRAIN DROP MANHOLE 47  
EXISTING APPROVED DESIGN  
EXHIBIT I

SCALE 1"=10'



JUAN TABO HILLS ESTATES STORM DRAIN MANHOLE 47 (NO DROP)  
PROPOSED REVISED DESIGN  
EXHIBIT II

SCALE 1"=10'

# Hydraulics of Circular Drop Manholes

F. Granata<sup>1</sup>; G. de Marinis<sup>2</sup>; R. Gargano<sup>3</sup>; and W. H. Hager, F.ASCE<sup>4</sup>

**Abstract:** Circular drop manholes are widely employed in steep urban drainage systems. Drop manholes may lead to poor hydraulic conditions if their energy dissipation is inadequate. The dominant hydraulic features of drop manholes depend on the flow regimes, characterized in terms of the dimensionless impact parameter. Depending on the latter parameter, the energy dissipation can vary within large limits, affecting thereby the downstream flow features. Also, the water pool depth inside the manhole and the air entrainment have been studied in terms of both the hydraulic and geometric parameters. Moreover, the conditions for which a drop manhole generates flow choking at its inlet or outlet have been investigated. Empirical equations for practical manhole design are provided. The importance of suitable manhole aeration is highlighted.

**DOI:** 10.1061/(ASCE)IR.1943-4774.0000279

**CE Database subject headings:** Air entrainment; Manholes; Energy dissipation; Experimentation; Sewers; Critical flow; Hydraulics.

**Author keywords:** Air entrainment; Choking; Drop manhole; Energy dissipation; Experimentation; Impact number; Sewer; Supercritical flow.

## Introduction

Drop manholes are ancient hydraulic structures, as testified by Roman aqueducts (Chanson 2002). Nowadays, they are widely implemented in drainage networks for steep urban catchments, where the topography induces excessive flow velocities. The presence of drops allows to release the design of sewer systems from the slope of urban areas, thereby decreasing pipes slope. The flow velocities are then reduced and thus consistent with adequate working conditions of sewers.

A minimum drop height to avoid negative backwater effects to the manhole is required (Christodoulou 1991), and choking of the downstream sewer should be avoided (De Martino et al. 2002). In addition, a drop should generate a sufficient energy loss (e.g., Camino et al. 2009; de Marinis and Vicinanza 1994; Calomino et al. 1999). If the drop manhole has a poor energy dissipation, the kinetic energy at the manhole outlet will be larger than at the manhole inlet (Rajaratnam et al. 1997; Chanson 2004). If the energy losses are significant, the flow depth in the downstream sewer may be higher than upstream of it, causing choking of the outflow (Christodoulou 1991). Therefore, adequate dropshaft de-

sign has to take into account two aspects: (1) significant reduction of kinetic energy and (2) optimum flow conditions, particularly in terms of choking.

The hydraulic performance of drop manholes depends on the approach flow characteristics, the manhole geometry and the tail-water features. Despite a wide usage of drop manholes, this hydraulic structure has not yet been systematically studied. Therefore, an experimental research was initiated to study the performance of circular drop manholes under supercritical approach flow. The experimental facility allowed for analyzing a wide range of working conditions, taking into account the various factors controlling the performance of drop manholes. The particular geometry of circular dropshaft has led to an improved classification of flow regimes as compared to Chanson (2004), to understand their basic behavior. On the basis of these regimes, the manhole pool height is described. Furthermore, both the energy loss across the manhole and the residual energy head were investigated. Choking of the manhole outlet has also been studied using a novel dimensionless parameter. Finally, drop manholes may induce strong air flows, a feature addressed below. The results are compared with those of Chanson (2004), Granata (2007), and Rajaratnam et al. (1997). The present observations indicate that a poor hydraulic performance may result if a suitable aeration is absent, resulting for instance in excessive manhole pool depth or choking of the manhole outlet.

<sup>1</sup>Research Fellow, Dipartimento di Meccanica Strutture Ambiente e Territorio, Università di Cassino, Via G. Di Biasio 43, 03043 Cassino (FR), Italy (corresponding author). E-mail: f.granata@unicas.it

<sup>2</sup>Full Professor, Dipartimento di Meccanica Strutture Ambiente e Territorio, Università di Cassino, Via G. Di Biasio 43, 03043 Cassino (FR), Italy. E-mail: demarinis@unicas.it

<sup>3</sup>Associate Professor, Dipartimento di Meccanica Strutture Ambiente e Territorio, Università di Cassino, Via G. Di Biasio 43, 03043 Cassino (FR), Italy. E-mail: gargano@unicas.it

<sup>4</sup>Professor, Laboratory of Hydraulics, Hydrology and Glaciology VAW, ETH Zurich, CH-8092 Zürich, Switzerland. E-mail: hager@vaw.baug.ethz.ch

Note. This manuscript was submitted on September 23, 2009; approved on July 13, 2010; published online on July 16, 2010. Discussion period open until July 1, 2011; separate discussions must be submitted for individual papers. This paper is part of the *Journal of Irrigation and Drainage Engineering*, Vol. 137, No. 2, February 1, 2011. ©ASCE, ISSN 0733-9437/2011/2-102-111/\$25.00.

## Experimental Setup

The experiments were conducted at *Laboratorio di Ingegneria delle Acque*, Cassino University, Italy. The experimental facility consisted of plexiglass circular manhole models connected to a recirculation system (Fig. 1). The tests were performed using two different manhole models (Fig. 2): Model 1 of internal manhole diameter  $D_M=1$  m was tested with drop heights of  $s=0.5, 1.0, 1.5$ , and  $2.0$  m and the water discharge  $Q$  varied from 3 to 80 L/s. Model 2 had the characteristics  $D_M=0.48$  m,  $s=1.0, 1.2$ , and  $1.5$  m, and  $1.5 \text{ L/s} \leq Q \leq 60 \text{ L/s}$ . A jet box (e.g., Gargano and

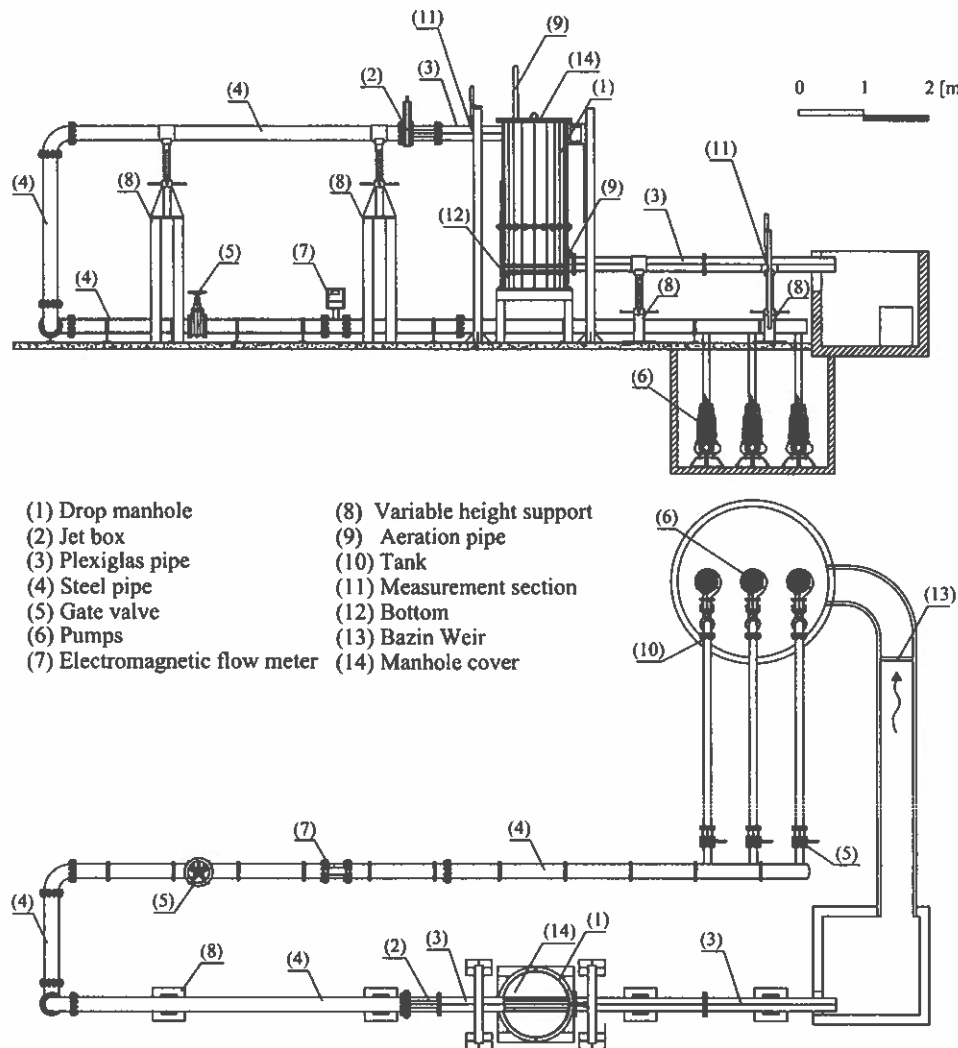


**Fig. 1.** Experimental facility

Hager 2002) placed upstream of the manhole controlled the approach (subscript  $a$ ) flow Froude number  $F_a$  and flow depth  $h_a$ . This device consists of a plexiglass frame in which plates of various filling ratios can be inserted.

Both the inlet (subscript in) and the outlet (subscript out) plexiglass pipes had a diameter of  $D_{in}=D_{out}=200$  mm, while the manhole bottom was plane. Flow depths were measured with piezometers and point gauges of  $\pm 0.5$  mm reading accuracies, and



**Fig. 2.** Experimental facility (a) side view ( $D_M=1.0$  m); (b) manhole model with  $D_M=0.48$  m

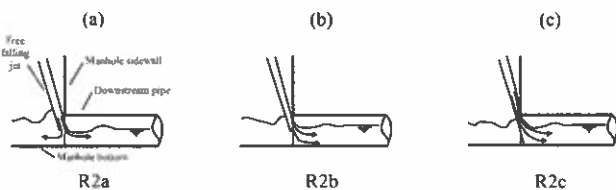


**Fig. 3.** Regime R2 with subregimes

the discharges were measured with an electromagnetic meter to  $\pm 0.1 \text{ L/s}$ . The approach flow depth  $h_o$  was recorded downstream of the jet box, where the flow has a horizontal surface and the pressure distribution is hydrostatic. The downstream (subscript  $d$ ) flow depth  $h_d$  was measured 3.4 m from the manhole outlet, where the flow is gradually varied and the air entrained by the drop manhole has almost detrained, resulting essentially in black water flow. The time-averaged pool (subscript  $p$ ) depth  $h_p$  was measured by a set of piezometers connected to the manhole bottom.

Air demand tests were performed sealing hermetically the manhole against the atmosphere using a plexiglass cover on the manhole top, so that the air was supplied only through a 60-mm diameter pipe placed on the dropshaft top. An anemometric probe was placed inside the pipe to measure the mean air flow velocity in a predefined sampling time. Preliminary tests indicated that a sampling time of 10 min assured adequate test accuracy and repeatability. Overall, more than 2,000 tests were performed.

## Flow Patterns

Different flow patterns occur in manhole flow depending on the hydrodynamic features of the approach and tailwater flows and the manhole geometry. The hydraulic behavior of a dropshaft depends strongly on the location of jet impact inside the manhole. Chanson (2002, 2004) described three basic flow patterns for the rectangular dropshaft, namely, Flow Regimes R1, R2, and R3 for subcritical approach flow. His classification will be extended in

the following to account for additional effects present for circular drop manholes. Experimentation has evidenced various forms of Regimes R2 and R3, urging to the definition of subregimes. These include

- Regime R1 occurs for small discharges, with the free jet plunging onto the shaft pool.
- Regime R2 includes conditions in which the jet impacts the manhole outlet zone.
- In Regime R2a [Fig. 3(a)], the falling jet impacts the zone between the manhole bottom and the outlet, with a flow portion directed to the downstream pipe, whereas the remainder feeds the manhole pool, forming a roller in the jet axis upstream the impact zone. Two lateral standing waves are generated close to the manhole outlet.
- Regime R2b [Fig. 3(b)] occurs if the entire free falling jet hits the downstream sewer invert, spreading in the pipe and forming two swirling wings. Most of the jet is directed into the downstream pipe, resulting in less energy dissipation and higher tailwater velocity.
- Regime R2c [Fig. 3(c)] results from a falling jet partially impacting the manhole sidewall above the manhole outlet, while its lower part enters directly the downstream pipe. The latter is also characterized by high velocity, entraining large quantities of air. The bottom pool is affected by less mixing and the free surface is less undular than in Regime R2a.
- Regime R3 occurs if the falling jet impacts the opposite manhole sidewall. Two subregimes were defined, namely,
- Regime R3a [Fig. 4(a)], for which the gravity-affected flow generates a vertical water veil beyond impact, with a water curtain covering the manhole outlet leading to outflow contraction. The free falling jet keeps a compact core beyond impact.
- Regime R3b [Fig. 4(b)] establishes for high approach flow Froude numbers with the water jet spreading radially over the manhole wall. A spiralling flow runs along the manhole wall interfering for high discharges even with the approach flow jet.

These flow regimes may be solely characterized with the impact number

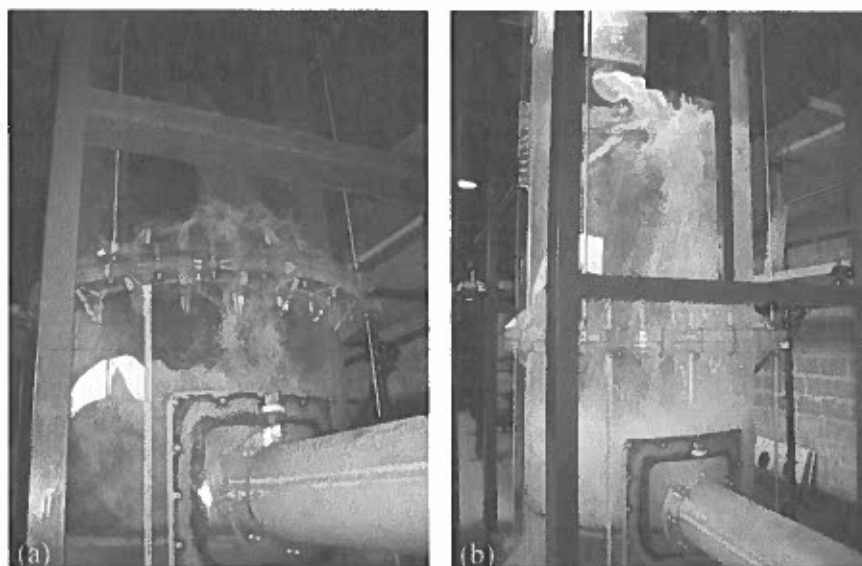


**Fig. 4.** Regime R3 in Model 1 with Regimes (a) R3a; (b) R3b

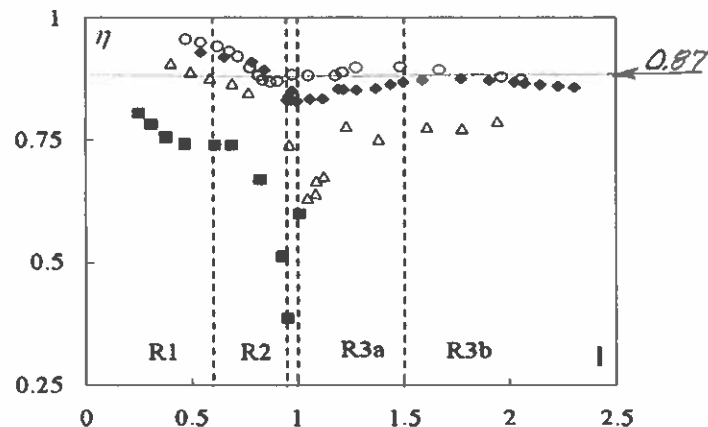


**Fig. 5.** Relative energy loss versus impact number  $\eta(I)$  for  $D_M = 1.0$  m and  $s[m] = 0.5$  (■), 1.0 (△), 1.5 (◆), and 2.0 (○), and jet-box plate of 50% (---) transitions among regimes

$$I = \left( \frac{2 \cdot s}{g} \right)^{0.5} \cdot \frac{V_o}{D_M} \quad (1)$$

where  $s$ =drop height;  $g$ =gravity acceleration; and  $V_o$ =approach flow velocity. It accounts for both the hydraulic approach flow features and the manhole geometry, relating the dimensionless drop height  $S=s/D_M$  to the velocity head  $V_o^2/(2g)$ . The impact number describes a free falling jet as a material point of velocity  $V_o$  (Granata et al. 2009). This parameter characterizes the regimes for supercritical approach flows because the impact number describes the ratio between the horizontal jet location and the manhole diameter. The present test data indicate that regime transitions can be approximated as  $I \approx 0.6$  between R1 and R2,  $I \approx 0.95$  to 1 between R2 and R3a, and  $I \approx 1.5$  between R3a and R3b.

## Energy Dissipation

### General

The head loss in drop manholes is caused by dissipative phenomena based on the increase of flow turbulence and jet spreading. For Regime R1, the energy dissipation is essentially due to the impact loss, given that the approach flow jet plunges into the manhole pool, inducing zones of large velocity gradients. Instead, for Regime R3, the energy dissipation is promoted by jet impact onto the manhole walls and by subsequent jet spreading, leading to the formation of spray and to a spiralling flow along the manhole wall. The latter dissipates energy by wall friction and plunging into the manhole pool along its boundaries. Further dissipative effects are related to manhole outflow. If the free falling jet impacts the downstream sewer invert, most of the discharge flows directly into the downstream pipe resulting in a small dissipative effect, causing unsatisfactory manhole operation with negative downstream flow features.

### Effect of Regime

Fig. 5 shows the typical results for the relative energy loss defined as

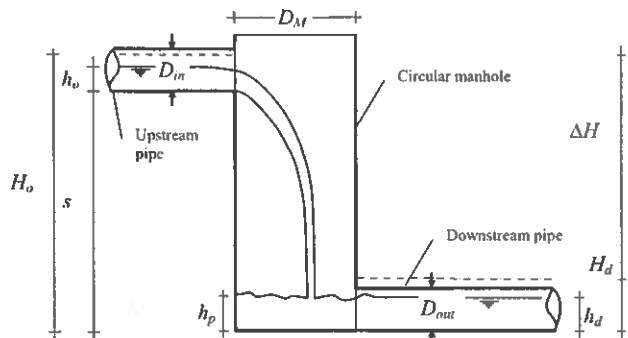


**Fig. 6.** Definition sketch for circular drop manhole

$$\eta = \frac{H_o - H_d}{H_o} \quad (2)$$

where  $H=s+h+V^2/2g$ =total energy head, i.e., with  $H_o=s+h_o+V_o^2/2g$  and  $H_d=h_d+V_d^2/2g$  (Fig. 6). For each flow regime, a trend in relative energy loss may be described. Regime R1 is characterized by the largest energy loss with the approach flow usually characterized by a low Froude number  $F_o = Q_o/(gD_o h_o^{1/2})^{1/2} \approx 1$ , i.e., small kinetic energy as compared to the drop height, such that  $\eta \rightarrow 0.9$ , depending on the drop height  $s$ . For Regime R2,  $\eta$  decreases notably passing through a minimum at the transition between Regimes R2 to R3. For Regime R2b, the falling jet impacts the downstream pipe invert generating a zone of large velocity gradients associated with only small energy dissipation. Additional energy is dissipated as the jet impacts the manhole sidewall. In Regime R3a, the energy loss increases with  $I$  due to jet impact against the opposite manhole wall jet deflection results, associated with an increased zone of large velocity gradients following impact onto the pool. Regime R3b, in turn, is characterized by a large energy loss due to dissipation related to jet spreading and subsequent plunging into the pool. However, as the impact number  $I$  increases,  $\eta$  appears to decrease. Fig. 5 shows that  $\eta$  generally decreases with the drop height  $s$ . For small  $s$ , the impact jet velocity is small, and the zone of large velocity gradients is confined.

### Effect of Manhole Diameter

Fig. 7 relates to the effect of manhole diameter reduction. In Regime R2, the relative energy dissipation decrease is less significant as the manhole diameter reduces. In addition, for  $D_M = 0.48$  m, the relative energy loss in Regime R3 is generally decreasing with  $I$ . The small  $\eta$  values for  $D_M = 1$  m under Regime R2 [Figs. 7(a and b)] and for  $D_M = 0.48$  m under Regime R3 for large approach flow filling ratio [Fig. 7(b)] indicate that  $H_o$  related to the drop height is only partly lost. The nondissipated portion is converted into kinetic energy in the downstream pipe. The maximum downstream energy head in the range  $0 < (H_o - s)/s < 0.6$  is (Granata et al. 2009)

$$\frac{H_d}{s} = 0.05 + 1.5 \frac{H_o - s}{s} \quad (3)$$

Eq. (3) indicates that the maximum of  $H_d$  depends mainly on the approach flow energy head  $H_o$ .

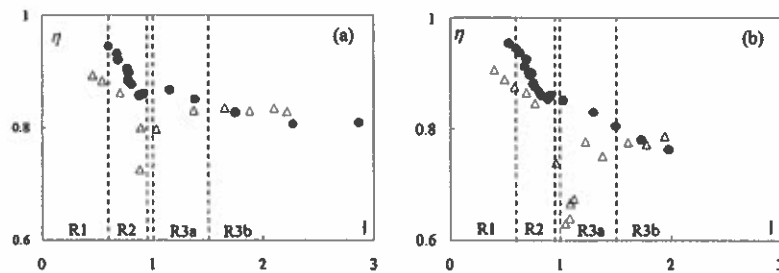


**Fig. 7.** Relative energy loss versus impact number  $\eta(l)$  for  $D_M[m]=1.0$  ( $\Delta$ ) and 0.48 ( $\bullet$ ), drop height  $s=1.0$  m and jet-box plate of (a) 40%; (b) 60%

### Loss Coefficient

In sewer design, the local head loss induced by a drop manhole is generally estimated independent of flow regime by

$$\Delta H = K \frac{V_o^2}{2g} \quad (4)$$

where the head loss coefficient  $K$  depends on the impact number  $l$  in the range  $0 < l^{-2} < 6$  as (Fig. 8)

$$K = \alpha \cdot l^{-2} \quad (5)$$

Eq. (5) expresses the main hydraulic features of drop manholes. The coefficient  $\alpha$  depends on the ratio  $D_M/s$  as (Fig. 9)

$$\alpha = 4.13 \cdot (D_M/s)^{-2.13} \quad (6)$$

Eqs. (5) and (6) lead to an average value of  $K$  for typical drop-shaft operating conditions

$$K = 2.06 \frac{s^{1.13}}{D_M^{0.13}} \frac{g}{V_o^2} \quad (7)$$

resulting in a mean relative head loss of

$$\frac{\Delta H}{s} = 1.03 \cdot \left( \frac{s}{D_M} \right)^{0.13} \quad (8)$$

Eq. (8) indicates that the head loss in a drop manhole is larger than the drop height if  $s > D_M$ , even if the actual energy loss depends on the manhole operating conditions.

Christodoulou (1991), in his experimentation on circular drop manholes, evaluated the local energy loss coefficient as a function of the drop parameter  $D = (gs)^{0.5}/V_o$ , resulting for  $D < 1.5$  in

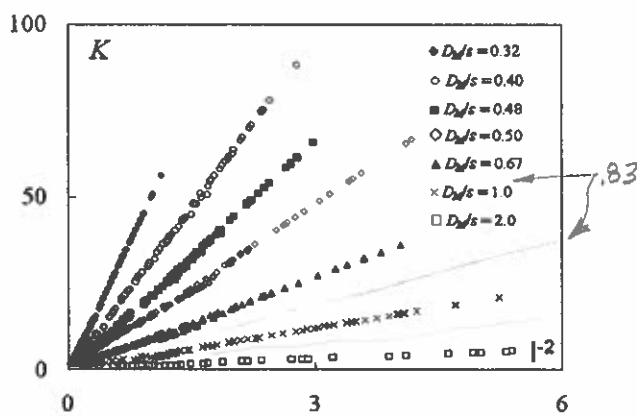


**Fig. 8.** Head loss coefficient  $K$  versus  $l^{-2}$

$$K = 0.20 + 2.30 \cdot D^{2.25} \quad (9)$$

The present test data lead to the slightly different relation

$$K = 0.25 + 2 \cdot D^2 \quad (10)$$

Whereas Eq. (9) only includes the range  $0 < D < 1.5$  [Fig. 10(b)], Eq. (10) fits the test data for  $0 < D < 8$  [Fig. 10(a)]. In addition, if  $D=0$  (i.e.,  $s=0$ ), Eq. (10) leads to  $K=0.25$ , in agreement with Gargano (2003) for head losses in through-flow manholes with  $s=0$ .

### Manhole Pool Height

The manhole pool (subscript  $p$ ) height  $h_p$  has to be predicted for a given discharge because of undesired backwater effects. The manhole drop height  $s$  has to be larger than the pool height for storm water flows, therefore, because the approach flow would be submerged otherwise, and the manhole does no more work under fully aerated flow conditions. Fig. 11 shows the ratio  $h_p/D_{out}$  versus  $l$  for fully aerated flow. In Regime R1, the pool height is unaffected by the upstream filling ratio. In Regime R2, the pool height increases, while in Regime R3a, small variations are observed. However, a remarkable increase is observed under Regime R3b. The effects of the approach flow depth  $h_o$  and of jet shape become important at the transition from Regime R2 to R3.

By momentum considerations for Regimes R1 and R2, the ratio  $h_p/D_{out}$  may be demonstrated to depend on the ratio  $Q^*/y_o^{0.7}$ , where  $Q^* = Q/(gD_{out}^3)^{0.5}$  is the manhole Froude number. An analysis of the test data for Regimes R1 and R2 results in (Fig. 12)

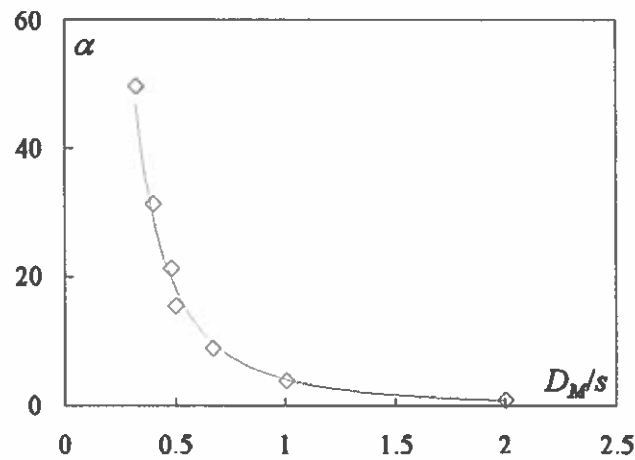


**Fig. 9.** Coefficient  $\alpha$  versus ratio  $D_M/s$

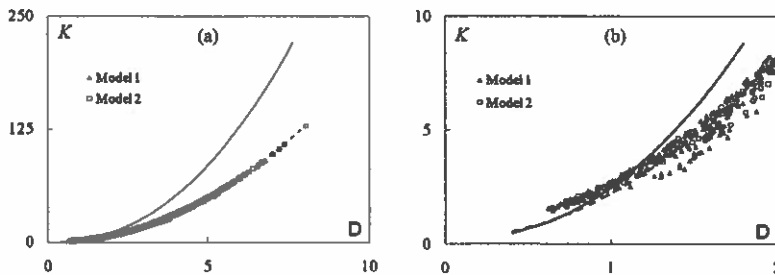


**Fig. 10.** Local energy loss coefficient versus drop parameter  $K(D)$  (a) entire present test range; (b) test data for  $0 < D < 2$  with Eq. (9) (—), Eq. (10) (---)

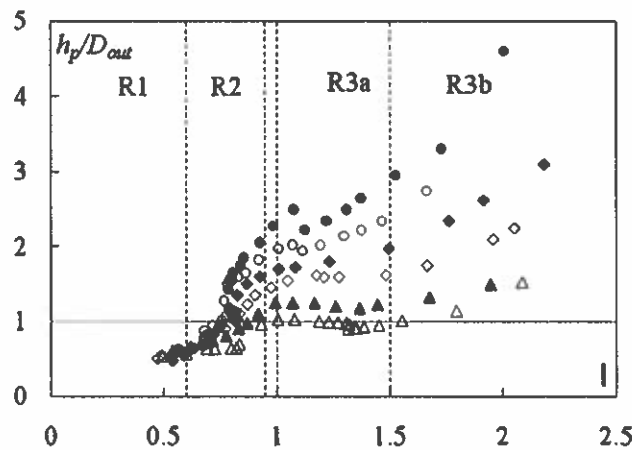


**Fig. 11.** Pool height  $h_p/D_{out}$  versus  $l$  for  $D_M=1.0$  m,  $s=2.0$  m, and jet-box opening of 30 ( $\Delta$ ), 40 ( $\blacktriangle$ ), 50 ( $\diamond$ ), 60 ( $\blacklozenge$ ), 70 ( $\circ$ ), and 80% ( $\bullet$ )

$$\frac{h_p}{D_{out}} = 0.3 + \left(1 + \frac{s}{D_M}\right) \frac{Q^*}{y_o^{0.7}} \quad (11)$$

Eq. (11) indicates that for Regimes R1 and R2, the relative pool height depends on both the relative drop height  $s/D_M$  and on the jet shape expressed by  $Q^*/y_o^{0.7}$ .

If the manhole operates under Regime R3 (for which normally  $h_p/D_{out} > 1.3$ ), the drop manhole outflow is similar to orifice flow. Energy considerations lead to

$$\frac{h_p}{D_{out}} = 0.6 + \left(7.3 - \frac{D_M}{D_{out}}\right) \cdot Q^* \quad (12)$$

Eq. (12) indicates that in Regime R3 (Fig. 13), the relative pool height depends on the discharge and the ratio  $D_M/D_{out}$ , yet not on the approach flow filling ratio.

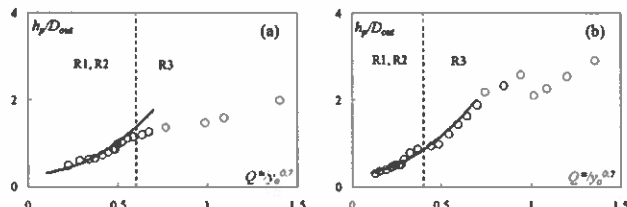


**Fig. 12.** Manhole pool height  $h_p/D_{out}$  versus  $Q^*/y_o^{0.7}$  for (a)  $D_M=1.0$  m,  $s=2.0$  m, and plate of 45%; (b)  $D_M=0.48$  m,  $s=1.0$  m, and plate of 80%. Test data ( $\circ$ ) with Eq. (11) (—)

## Flow Choking

Choking of pipe flow corresponds to a sudden and abrupt transition from free surface to pressurized flow. This phenomenon has received scarce attention until now, despite its relevance for overcharged sewers. As pointed out by Hager (1999), the effect of the approach flow conditions is essential and manhole outflows subjected with a supercritical approach flow may undergo dangerous features mainly because of shock wave generation. The presence of manholes significantly affects the choking phenomena in a sewer system. Choking downstream of manholes may be developed by

- Touching of sewer vertex by a wave maximum;
- Cut down of air transport;
- Breakdown of supercritical flow structure;
- Development of moving hydraulic jumps; and
- Abrupt transition from free surface to pressurized sewer flow.

For supercritical flow, the sewer filling ratio has to be limited sufficiently below the soffit. The sewer inflow downstream of a manhole may choke if the filling ratio is too large. In a sewer manhole, the transition from free surface to pressurized pipe flow is often characterized by the capacity (subscript  $C$ ) pipe Froude number (Hager 1999)  $F_C = Q_C / (g D^5)^{0.5}$ . Sewer choking was previously studied relative to abrupt cross-sectional manhole changes (Gargano and Hager 2002), bend manholes (Del Giudice et al. 2000), and junction manholes (Gisonni and Hager 2002).

As for drop manholes, De Martino et al. (2002) performed tests for small relative drops ( $s/D \leq 1$ ) proposing a choking condition depending on the filling ratio  $y_o$ , the ratio  $s/D$ , and on  $F_C$ . Choking downstream of a drop manhole with  $s/D > 2$  is a complex phenomenon affected by many factors. A functional dependence between  $F_C$  and the approach flow filling ratio has not been found. The test data indicate the importance of the manhole pool height. The pool blocks the air flow from the manhole to the downstream pipe as its level increases. Moreover, experimentation indicates that downstream flow choking is also affected by

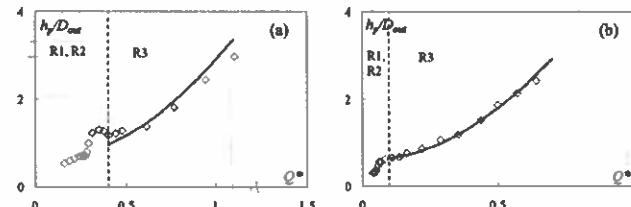


**Fig. 13.** Manhole pool height  $h_p/D_{out}$  versus  $Q^*$  for (a)  $D_M=1.0$  m,  $s=1.5$  m, and plate of 40%; (b)  $D_M=0.48$  m,  $s=1.5$  m, and plate of 85%. Test data ( $\diamond$ ) with Eq. (12) (—)

the approach flow Froude number  $F_o$  (Hager 1999), and the approach flow filling  $y_o = h_o/D$ . A data analysis demonstrates that choking can be predicted by the combined parameter  $\psi = y_o [F_{och} - (h_p/D_{out})]$ , where  $F_{och}$  = approach flow Froude number for choking inception (subscript ch). In Fig. 14,  $\psi$  is plotted versus  $y_o$ , from which

$$\psi_{ch} = -5.9y_o + 3.5 \quad (13)$$

tested for  $0.3 < y_o < 0.75$ . Eq. (13) splits the plane ( $y_o, \psi$ ) into a "choking zone" and a "no choking zone" (Fig. 14). These results relate to aerated manhole flow. Below, the effect of aeration absence on choking inception is also discussed.

Eq. (13) allows to verify the choking risk of a downstream sewer. First, determine the approach flow filling ratio  $y_o$  and the Froude number  $F_o$ . Then, evaluate  $h_p/D_{out}$  from Eq. (11) or Eq. (12), and finally the parameter  $\psi' = y_o [F_{och} - (h_p/D_{out})]$ . Compare the value of  $\psi'$  to  $\psi_{ch}$  from Eq. (13). If  $\psi' > k \cdot \psi_{ch}$ , where  $k$  is a suitable safety factor, the verification is satisfied.

## Air Entrainment

Hydraulic structures may undergo a strong interaction between water and air flows (Falvey 1980), including drop manholes (Rajaratnam et al. 1997; Chanson, 2004; or Granata, 2007). In a circular drop manhole, both local and continuous air entrainment and entrapment processes are observed. These phenomena essentially depend on the manhole operating regime. In particular, the following mechanisms may occur:

- Entrainment by free falling jet;
- Jet plunging into manhole pool, if jet does not impact the opposite manhole wall;
- Air entrainment mechanism due to water veil along manhole wall and plunging into the manhole pool along the boundaries after jet impact onto the opposite wall;
- Entrainment due to droplets originating from jet breakup subsequent to jet impact onto wall; and
- Surface entrainment at manhole pool surface and supercritical downstream flow.

These phenomena induce an air flow both as entrained air bubbles and as air venting above the water surface. The latter may be considerable as compared to the entrained air (Edwini-Bonsu and Steffler 2006; Granata 2007).

Only a portion of the entrained air is transported into the downstream pipe, representing the actual manhole air demand

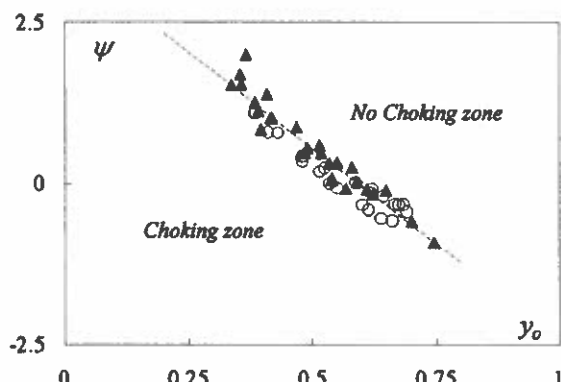


**Fig. 14.** Choking inception from Model 1 ( $\blacktriangle$ ), Model 2 ( $\circ$ ), with Eq. (13) (---)

from the atmosphere. The remaining portion is released in the dropshaft by detrainment and can be reentrained by water flow. Fig. 15(a) shows typical results of the manhole air (subscript air) demand data, where the ratio  $\beta = Q_{air}/Q$  is plotted versus  $l$ . In Regime R1,  $\beta$  increases rapidly with  $l$ . The glassy appearance of the free falling jet indicates that there is no surface entrainment. In Regime R2b,  $\beta$  reaches its maximum value. In Regime R2c, an abrupt drop of air demand from outside is generally observed, due to submergence of the manhole outlet or jet spreading. These involve an air seal of the manhole outlet, avoiding direct ventilation from the manhole. In Regime R3a, a second peak of  $\beta$  is generally observed, while in R3b,  $\beta$  decreases with  $l$ . Then, the breakup due to jet impact on the opposite manhole wall generates considerable spray.

Two aeration regimes may be considered [Figs. 15(b and c)]

- Aeration Regime I with a direct ventilation of the downstream pipe from the manhole.
- Aeration Regime II if downstream pipe ventilation is cut down by outlet submergence or jet spreading.

Fig. 16 shows the typical air demand for three investigated drop heights. A small drop height results in a smaller air demand peak for both aeration regimes, due to lower velocity at the jet impact point. The kinetic energy of the free falling jet becomes smaller as the drop height decreases, leading to a less effective air entrainment action.

The relevance of air flow peak observed in Aeration Regime I may lead to improved aeration for small discharges, a desirable effect for combined sewer systems, promoting sewage oxygen-

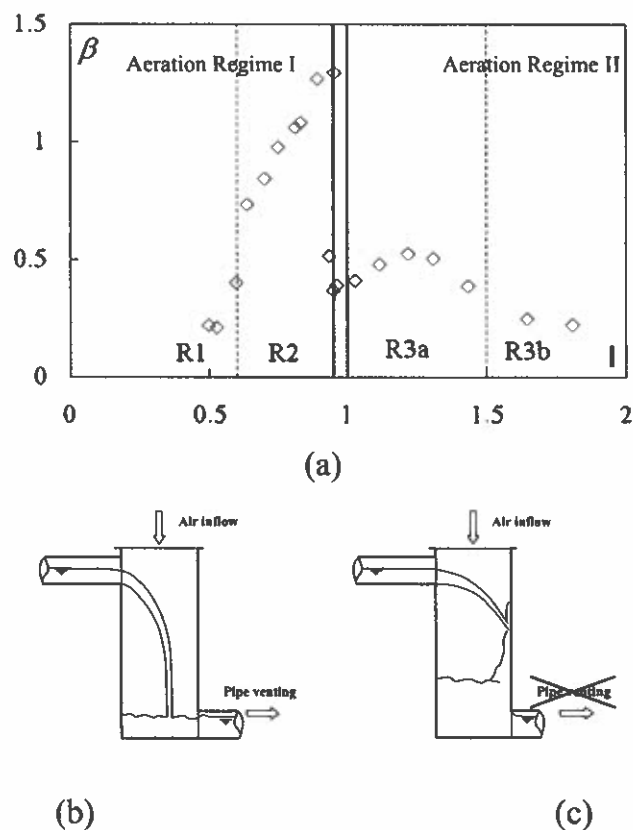


**Fig. 15.** (a) Relative air demand  $\beta = Q_{air}/Q$  versus  $l$  for  $D_M = 1.0$  m,  $s = 1.5$  m, and jet-box opening of 60%; sketch of (b) Aeration Regime I; and (c) Aeration Regime II

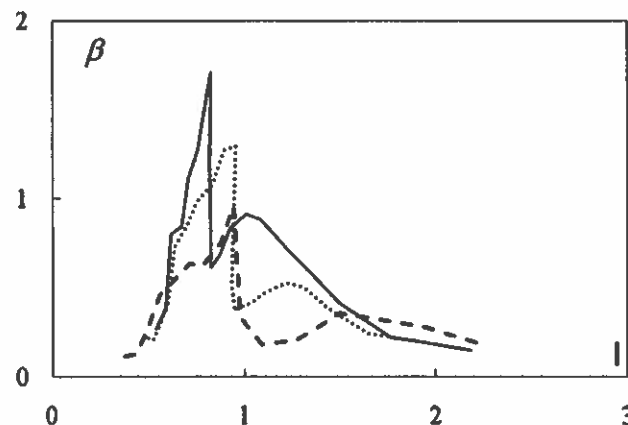


Fig. 16. Relative air demand  $\beta = Q_{\text{air}}/Q(l)$  for  $D_M = 1.0$  m,  $s$  [m] = 2.0 (—), 1.5 (···), and 1.0 (---), and jet-box opening of 60%

ation. To provide an estimate of the maximum air demand under all possible operating conditions, a data analysis indicated that maximum values depend on the two parameters  $ly_o^{0.5}$ , and  $\beta y_o^{0.5}/F_o$ . Fig. 17 shows that the maximum (subscript max) air demand for Aeration Regime I follows for  $ly_o^{0.5} < 0.4$  by

$$(\beta y_o^{0.5}/F_o)_{\max} = 5 \cdot ly_o^{0.5} - 0.5 \quad (14)$$

whereas for Aeration Regime II, the upper limit is given for  $0.4 < ly_o^{0.5} < 3$  by

$$(\beta \cdot y_o^{0.5}/F_o)_{\max} = \exp(-1 \cdot y_o^{0.5}) \quad (15)$$

Eqs. (14) and (15) give the upper envelopes of the dimensionless air demand values. Eq. (14) indicates that in Regime I, the maximum air demand  $\beta$  increases with  $ly_o^{0.5}$  following a linear trend. The effects of jet shape and velocity  $V_o$  for the air entrainment are evident. In Regime II,  $\beta$  decreases following an exponential trend. This is due to two factors:

- Jet spreading along the manhole wall leads to a reduced plunging velocity.
- As the manhole pool depth increases, buoyancy adds to the entrainment forces acting on air bubbles. Therefore, the latter are not transported into the downstream pipe, and air is released in the manhole.

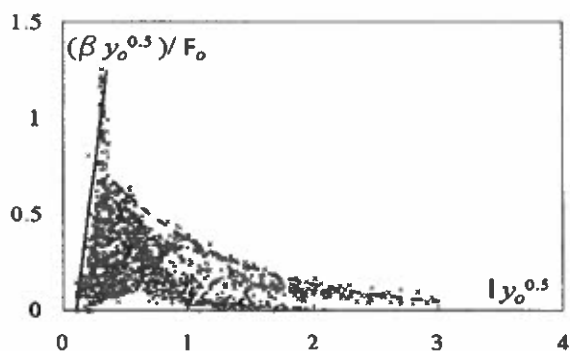


Fig. 17. Upper limit of relative air demand for Aeration Regimes I (—) and II (---). Test data from Model 1 (●) and Model 2 (×)

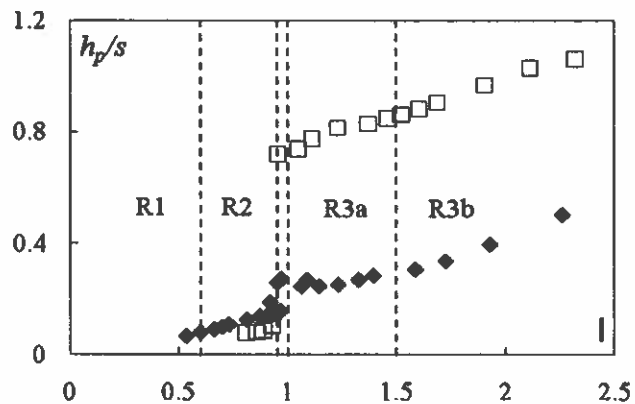


Fig. 18. Effects of air supply absence on relative pool height  $h_p/s(l)$ . Test data for aerated (◆) and unaerated (□) conditions for  $D_M = 1.0$  m,  $s = 1.5$  m, and jet-box opening of 70%

### Absence of Aeration

The performance of a drop manhole may be strongly influenced by the air supply. If the air entrained and transported in the downstream pipe is not supplied from the atmosphere, a negative pressure inside of the manhole is set up, inducing an abrupt manhole pool height increase. Fig. 18 compares  $h_p/s(l)$  in the presence and absence of manhole air supply, for Model 1 and  $s = 1.5$  m. Note the abrupt increase in correspondence with Regime R2c. Unfortunately, the absence of suitable air supply is frequent in real sewer systems, because generally the sewer is not equipped with specific air supply devices. For small drop heights ( $h_p/s \geq 1$ ), a pool increase to above the manhole intake elevation may induce undesired backwater effects to the upstream sewer (Figs. 18 and 19).

Moreover, if a drop manhole has no air supply, the risk of downstream flow choking increases. The enhanced cut down of air flow toward the downstream pipe and the higher pool depth due to the negative pressure inside the manhole lead to the onset of choking prior than for aerated manholes. Tests confirmed that the absence of air supply is disadvantageous in terms of the choking risk. For a given approach flow, the average manhole pool level may be so high that  $(y_o, \psi)$  is located in the choking zone in the absence of air supply, as shown in Fig. 20. Tests further indi-



Fig. 19. Submerged manhole inlet flow in absence of air supply

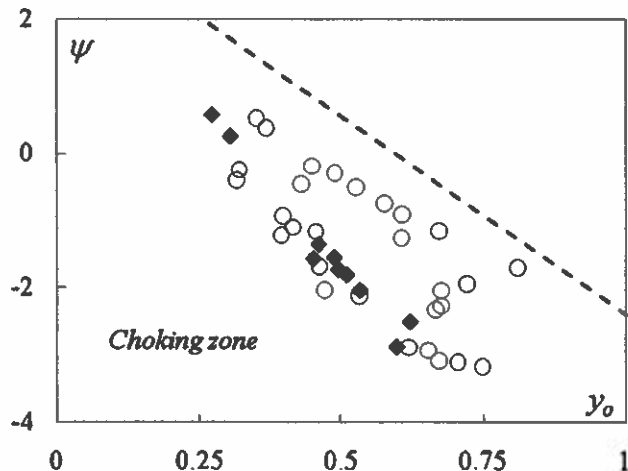


**Fig. 20.** Effect of air supply absence on choking inception. Test data for Model 1 ( $\blacklozenge$ ) with  $s[m]=1.5$  and 2.0, and Model 2 (O) with  $s[m]=1.0$ , 1.2, and 1.5, with Eq. (13) (---)

cated that the parameter  $\psi$  is less effective to predict the choking onset than for manholes with an air supply, because the choking onset condition may not be well defined (Fig. 20).

### Design Example

Based on the previous results, a practical application is illustrated in the following. Assume that a steep urban sewer including drop manholes has been designed based on: design discharge  $Q=135 \text{ l/s}$ , inlet and outlet pipe diameter  $D_{in}=D_{out}=300 \text{ mm}$ , pipe invert slope  $S_f=0.09$ , Manning's roughness coefficient  $n=0.014 \text{ m}^{-1/3} \cdot \text{s}$ , manhole diameter  $D_M=1.2 \text{ m}$ , and drop height  $s=0.8 \text{ m}$ . Under these conditions, the uniform flow conditions are  $y_o=0.5$ ,  $V_o=3.74 \text{ m/s}$ ,  $F_o=3.4$ , and  $I=1.26$ , and the manhole operates in Regime R3a from Eq. (1). It would seem to be an acceptable design. However, the pool height is  $h_p=0.91 \text{ m}$  from Eq. (12), larger than the drop height, with a risk of backwater effects, while the choking verification would not be satisfied, given that  $\psi'=0.204 < \psi_{ch}=0.55$  from Eq. (13). A drop height increase to  $s=1.2 \text{ m}$  combined with a manhole diameter increase to  $D_M=1.6 \text{ m}$  leads to  $h_p=0.61 \text{ m}$  and to  $\psi'=0.69 > 1.2 \cdot 0.55 = 0.66$  (with 1.2 as safety factor), so as to avoid undesired backwater effects and choking inception. Obviously, a drop height increase allows to reduce the number of drop manholes. Moreover, for such a manhole, the local head loss coefficient is  $K=1.68$  from Eqs. (5) and (7), while the maximum relative air demand is  $\beta=Q_{air}/Q=2.14$  from Eq. (15).

### Conclusions

Drop manholes constitute a standard hydraulic device of drainage networks in steep urban catchments, to reduce flow velocities. This research presents results relative to the circular-shaped drop manhole under supercritical approach flow conditions using hydraulic experimentation and a data analysis. The following main results were found:

- Energy dissipation was studied relative to the variation of the downstream energy head, resulting in expressions for the en-

ergy loss. Operating conditions (i.e., Regime R2) leading to small energy dissipation should be avoided.

- Manhole pool level was investigated and two empirical equations in terms of relative drop height and discharge are proposed.
- A novel parameter to characterize choking inception in the manhole downstream pipe was introduced, taking into account the relative drop height and the approach flow conditions.
- Air entrainment mechanisms of manhole jet flow were examined along with the manhole main aeration conditions. Estimates for the maximum air demand have been proposed.
- Effects of the absence of external air supply are discussed, pointing at the high risk of poor hydraulic performance along with a breakdown of the supercritical flow structure.

This study highlights that the optimum hydraulic performance of a drop manhole is affected by many hydraulic and geometric parameters. The relations provided are considered useful to improve drop manholes design.

### Acknowledgments

The writers would like to thank Engr. Tiziana Calcagni for having performed selected experimental tests.

### Notation

The following symbols are used in this paper:

$D$	= pipe or manhole diameter;
$D$	= drop number;
$F$	= Froude number;
$g$	= gravitational acceleration;
$H$	= energy head;
$h$	= flow depth;
$I$	= impact number;
$K$	= local energy loss coefficient;
$k$	= choking safety factor;
$n$	= Manning's roughness coefficient;
$Q$	= discharge;
$Q^*$	= nondimensional discharge;
$S$	= dimensionless drop height;
$s$	= drop height;
$V$	= flow velocity;
$y$	= pipe flow filling ratio;
$\alpha$	= coefficient correlating $K$ and $I$ ;
$\beta$	= air supply coefficient;
$\eta$	= relative energy loss; and
$\psi$	= choking parameter.

### Subscripts

Air	= air;
C	= capacity;
ch	= choking inception;
d	= downstream;
in	= inlet;
M	= manhole;
o	= approach flow;
out	= outlet; and
p	= pool.

## References

- Calomino, F., Frega, G., Piro, P., and Gironda Veraldi, M. (1999). "Hydraulics of drops in supercritical flow." *8th Int. Conf. Urban Storm Drainage*, Sydney, Australia, 2139–2146.
- Camino, G. A., Zhu, D. Z., Rajaratnam, N., and Shome, M. (2009). "Use of a stacked drop manhole for energy dissipation: A case study in Edmonton, Alberta." *Can. J. Civ. Eng.*, 36(6), 1037–1050.
- Chanson, H. (2002). "An experimental study of Roman dropshaft hydraulics." *J. Hydraul. Res.*, 40(1), 3–12.
- Chanson, H. (2004). "Hydraulics of rectangular dropshafts." *J. Irrig. Drain. Eng.*, 130(6), 523–529.
- Christodoulou, G. C. (1991). "Drop manholes in supercritical pipelines." *J. Irrig. Drain. Eng.*, 117(1), 37–47.
- Del Giudice, G., Gisonni, C., and Hager, W. H. (2000). "Supercritical flow in bend manhole." *J. Irrig. Drain. Eng.*, 126(1), 48–56.
- de Marinis, G., and Vicinanza, D. (1994). "Sul comportamento idraulico di salti di fondo in corrente ipercritica [On hydraulic behavior of supercritical flow across bottom drops]." *XXIV Convegno di Idraulica e Costruzioni Idrauliche*, Naples, Italy, 1(T2), 123–136 (in Italian).
- De Martino, F., Gisonni, C., and Hager, W. H. (2002). "Drop in combined sewer manhole for supercritical flow." *J. Irrig. Drain. Eng.*, 128(6), 397–400.
- Edwini-Bonsu, S., and Steffler, P. M. (2006). "Modeling ventilation phenomenon in sanitary sewer systems: A system theoretic approach." *J. Hydraul. Eng.*, 132(8), 778–790.
- Falvey, H. T. (1980). *Air-water flow in hydraulic structures, Engineering monograph No. 41*, U.S. Bureau of Reclamation, Denver.
- Gargano, R. (2003). "Effetti indotti dai pozzetti di ispezione sulle correnti ipercritiche [The influence of sewer manholes on supercritical flows]." *L'Acqua*, 6, 25–31 (in Italian).
- Gargano, R., and Hager, W. H. (2002). "Supercritical flow across sewer manholes." *J. Hydraul. Eng.*, 128(11), 1014–1017.
- Gisonni, C., and Hager, W. H. (2002). "Supercritical flow in manholes with a bend extension." *Exp. Fluids*, 32(3), 357–365.
- Granata, F. (2007). "Hydraulics of circular drop manholes." Ph.D. thesis, Cassino Univ., Cassino, Italy.
- Granata, F., de Marinis, G., Gargano, R., and Hager, W. H. (2009). "Energy loss in circular drop manholes." *33rd IAHR Congress* (CD-ROM), Vancouver, Canada.
- Hager, W. H. (1999). *Wastewater hydraulics*, Springer, Berlin.
- Rajaratnam, N., Mainali, A., and Hsung, C. Y. (1997). "Observations on flow in vertical dropshafts in urban drainage systems." *J. Environ. Eng.*, 123(5), 486–491.

T1 JTH ESTATES SANDIA MAIN STORM DRAIN 0  
 T2 TIJERAS ARROYO TO JTH UNIT 1 EXISTING 84" STORM PIPE (FILE:JTH\_F.WSW)  
 T3 STARTING POINT AT MANHOLE 13- ASSUMING JHUGHES WSEL (2-24-17) 420.164  
 SO 1357.700 415.000 4 .013 .000 .000 1  
 R 1470.900 418.750 4 .013 .000 .000 1  
 JX 1480.900 419.250 7 5 .013 17.880 24.440 423.000 426.700 90.0-90.0 .000  
 R 1737.900 427.200 7 .013 .013 19.990 435.500 -90.0 .000 1  
 JX 1747.900 427.200 9 8 .013 .013 25.620 442.100 -90.0 .000 1  
 R 1982.900 432.500 9 .013 .013 41.950 437.400 -70.0 .000 1  
 JX 1992.400 432.700 11 10 .013 .013 .000 .000 1  
 R 2125.200 435.300 11 .013 .013 .000 .000 1  
 JX 2130.200 435.400 13 12 .013 .013 .000 .000 1  
 R 2147.900 438.600 13 .013 .013 .000 .000 1  
 JX 2157.900 438.700 14 .013 .013 .000 .000 1  
 R 2228.850 457.500 14 .013 .013 .000 .000 1  
 JX 2238.850 457.600 15 .013 .013 .000 .000 1  
 R 2447.850 459.970 15 .013 .013 259.120 459.970 459.970 45.0-45.0 .000  
 JX 2459.850 460.070 18 16 17.013 67.440 51.200 489.000 489.000 90.0-90.0 .000  
 R 2747.100 467.030 18 .013 .013 .000 20.000 1  
 R 3172.300 476.460 18 .013 .013 .000 15.000 1  
 R 3290.000 479.240 18 .013 .013 .000 .000 1  
 R 3386.260 482.940 18 .013 .013 .000 .000 1  
 JX 3394.260 483.040 21 19 20.013 46.040 51.200 489.000 489.000 90.0-90.0 .000  
 R 3432.000 485.570 21 .013 .013 .000 .000 1  
 JX 3438.000 485.670 23 22 .013 7.330 492.000 45.0 .000  
 R 3686.500 495.220 23 .013 .013 .000 10.000 1  
 R 4086.100 511.150 23 .013 .013 .000 10.000 1  
 R 4265.400 519.010 23 .013 .013 .000 5.000 1  
 JX 4271.400 519.110 25 24 .013 15.200 529.000 70.0 .000  
 R 4482.200 527.090 25 .013 .013 .000 .000 1  
 JX 4488.200 527.190 28 26 27.013 6.990 31.600 535.020 534.390 50.0-30.0 .000  
 R 4586.350 531.800 28 .013 .013 .000 -30.000 1  
 JX 4592.350 531.900 30 29 .013 26.830 540.000 -90.0 .000  
 R 4845.700 541.580 30 .013 .013 .000 40.000 1  
 R 5206.100 556.330 30 .013 .013 .000 .000 1  
 R 5562.500 570.750 30 .013 .013 .000 .000 1  
 SH 5562.500 570.950 30 .013 .013 .000 574.950 .000 .000 1  
 CD 1 4 2 .000 7.000 .000 .000 .000 .000 1  
 CD 2 2 0 .000 15.000 30.000 .000 .000 .000 1  
 CD 3 4 1 .000 7.500 .000 .000 .000 .000 1  
 CD 4 4 1 .000 7.500 .000 .000 .000 .000 1  
 CD 5 4 1 .000 2.000 .000 .000 .000 .000 1  
 CD 6 4 1 .000 2.000 .000 .000 .000 .000 1  
 CD 7 4 1 .000 7.000 .000 .000 .000 .000 1  
 CD 8 4 1 .000 2.000 .000 .000 .000 .000 1  
 CD 9 4 1 .000 7.000 .000 .000 .000 .000 1  
 CD 10 4 1 .000 2.000 .000 .000 .000 .000 1  
 CD 11 4 1 .000 7.000 .000 .000 .000 .000 1  
 CD 12 4 1 .000 2.500 .000 .000 .000 .000 1  
 CD 13 4 1 .000 7.000 .000 .000 .000 .000 1

REVISED HYDRAULICS FOR  
 SHEET SR

CD	14	4	1	.000	7.000	.000
CD	15	4	1	.000	7.000	.000
CD	16	4	1	.000	3.500	.000
CD	17	4	1	.000	6.000	.000
CD	18	4	1	.000	5.500	.000
CD	19	4	1	.000	2.000	.000
CD	20	4	1	.000	3.000	.000
CD	21	4	1	.000	4.500	.000
CD	22	4	1	.000	1.500	.000
CD	23	4	1	.000	4.500	.000
CD	24	4	1	.000	2.000	.000
CD	25	4	1	.000	4.500	.000
CD	26	4	1	.000	1.500	.000
CD	27	4	1	.000	2.500	.000
CD	28	4	1	.000	4.500	.000
CD	29	4	1	.000	2.000	.000
CD	30	4	1	.000	4.500	.000
Q				276.6660	.0	

## REVISED

## Hydrology Worksheet 5R

FILE: JTH.F.WSW

W S P G W - CIVILDESIGN Version 14.05

Program Package Serial Number: 1454

## WATER SURFACE PROFILE LISTING

JTH ESTATES SANDIA MAIN STORM DRAIN

Date: 2-27-2018 Time:11: 3:51

TIJERAS ARROYO TO JTH UNIT 1 EXISTING 84" STORM PIPE (FILE:JTH.F.WSW)

STARTING POINT AT MANHOLE 13- ASSUMING JHUGHES WSEL (2-24-17)

Station	Invert Elev	Depth (FT)	Water Elev	Q (CFS)	Vel (FPS)	Head	Energy Grd.EI.	Critical Depth	Flow Width	Top Dia.-FT or I.D.	Base Dia.-FT or I.D.	Wt ZL	No Wt Prs/Pip	Type Ch	
L/Elem	Ch Slope														
MH13	1357.700	415.000	4.749	419.749	918.29	31.13	15.05	434.80	.00	7.16	7.23	"N"	X-Fall1	ZR	
	113.200	.03311	-	-	-	-	-	-	-	-	-	-	.00	.00	1 .0
JUNCT STR	1470.900	418.750	4.886	423.636	918.29	30.13	14.10	437.73	.00	7.16	7.22	4.44	.013	.00	- PIPE
MH12	1480.900	419.250	4.754	424.004	875.97	31.48	15.39	439.39	.00	7.16	7.15	7.500	.000	.00	1 .0
	257.000	.03022	-	-	-	-	-	-	-	-	-	-	.00	.00	- PIPE
JUNCT STR	1737.900	427.000	4.823	431.823	875.97	30.98	14.90	446.73	.00	6.80	6.54	7.000	.000	.00	1 .0
MH11	1747.900	427.200	4.585	431.785	855.98	32.04	15.94	447.73	.00	6.78	6.66	7.000	.000	.00	- PIPE
	120.768	.02226	-	-	-	-	-	-	-	-	-	-	.00	.00	- PIPE
1868.668	429.924	4.427	434.351	855.98	33.36	17.29	451.64	.00	6.78	6.75	7.000	.000	.00	1 .0	
	114.232	.02226	-	-	-	-	-	-	-	-	-	-	.00	.00	- PIPE
1982.900	432.500	4.251	436.751	855.98	34.99	19.01	455.77	.00	6.78	6.84	7.000	.000	.00	1 .0	
JUNCT STR	1992.400	432.700	4.006	436.706	830.36	36.47	20.65	457.36	.00	6.75	6.93	7.000	.000	.00	- PIPE
MH10	67.583	.0196	-	-	-	-	-	.0409	.39	4.25	3.26	.013	.00	.00	- PIPE
	2059.983	434.023	3.862	437.885	830.36	38.13	22.58	460.46	.00	6.75	6.96	7.000	.000	.00	1 .0
	65.217	.0196	-	-	-	-	-	.0520	3.39	3.86	3.80	5.34	.013	.00	- PIPE



## JTH ESTATES SANDIA MAIN STORM DRAIN

TIJERAS ARROYO TO JTH UNIT 1 EXISTING 84" STORM PIPE (FILE:JTH\_F.WSW)  
 STARTING POINT AT MANHOLE 13- ASSUMING JHUGHES WSEL (2-24-17)

Station	Invert Elev	Depth (FT)	Water Elev	Q (CFS)	Vel (FPS)	Head	Energy Grd. El.	Super Elev	Critical Depth	Flow Dia. - FT or I.D.	Top Dia. - FT	Base Wt ZL	No Wth Prs/Pip	
L/Elem	Ch Slope	-	-	-	-	-	-	-	-	-	-	-	Type Ch	
2201.219	450.178	4.285	454.464	788.41	31.93	15.83	470.29	.00	6.70	6.82	7.000	.000	1 .0	
5.370	.2650	-	-	-	-	-	-	.0299	.16	4.29	2.96	2.33	.013	.00
2206.589	451.602	4.462	456.064	788.41	30.44	14.39	470.46	.00	6.70	6.73	7.000	.000	1 .0	
4.691	.2650	-	-	-	-	-	-	.0266	.12	4.46	2.74	2.33	.013	.00
2211.280	452.844	4.652	457.497	788.41	29.03	13.08	470.58	.00	6.70	6.61	7.000	.000	1 .0	
4.087	.2650	-	-	-	-	-	-	.0236	.10	4.65	2.52	2.33	.013	.00
2215.367	453.927	4.855	458.783	788.41	27.68	11.89	470.68	.00	6.70	6.45	7.000	.000	1 .0	
3.535	.2650	-	-	-	-	-	-	.0211	.07	4.86	2.32	2.33	.013	.00
2218.903	454.864	5.074	459.938	788.41	26.39	10.81	470.75	.00	6.70	6.25	7.000	.000	1 .0	
3.027	.2650	-	-	-	-	-	-	.0189	.06	5.07	2.13	2.33	.013	.00
2221.930	455.666	5.312	460.978	788.41	25.16	9.83	470.81	.00	6.70	5.99	7.000	.000	1 .0	
2.543	.2650	-	-	-	-	-	-	.0170	.04	5.31	1.94	2.33	.013	.00
2224.472	456.340	5.575	461.915	788.41	23.99	8.94	470.85	.00	6.70	5.64	7.000	.000	1 .0	
2.065	.2650	-	-	-	-	-	-	.0154	.03	5.58	1.75	2.33	.013	.00
2226.537	456.887	5.872	462.759	788.41	22.87	8.12	470.88	.00	6.70	5.15	7.000	.000	1 .0	
1.545	.2650	-	-	-	-	-	-	.0141	.02	5.87	1.56	2.33	.013	.00
2228.082	457.296	6.223	463.520	788.41	21.81	7.39	470.90	.00	6.70	4.40	7.000	.000	1 .0	
.768	.2650	-	-	-	-	-	-	.0134	.01	6.22	1.34	2.33	.013	.00

## JTH ESTATES SANDIA MAIN STORM DRAIN

TIJERAS ARROYO TO JTH UNIT 1 EXISTING 84" STORM PIPE (FILE:JTH\_F.WSW)

STARTING POINT AT MANHOLE 13- ASSUMING JHUGHES WSEL (2-24-17)

Station	Invert Elev	Depth (FT)	Water Elev	Q (CFS)	Vel (FPS)	Head	Energy Grd.EI.	Super Elev	Critical Depth	Flow Dia.-FT or I.D.	Base Wt ZL	No Wth Prs/Pip	X-Fall ZR	Type Ch	
L/Elem	Ch Slope														
2228.850	457.500	6.702	464.202	788.41	20.79	6.71	470.92	.00	6.70	2.83	7.000	.000	0.0	1 .0	
JUNCT STR	.0100	-	-	-	-	-	-	-	-	-	-	-	-	-	
MH47	2238.850	457.600	6.889	464.489	788.41	20.56	6.56	471.05	.00	6.70	1.75	7.000	.000	0.0	1 .0
	.0113	-	-	-	-	-	-	.0135	.14	6.70	1.00	.013	.00	PIPE	
2261.738	457.860	7.000	464.860	788.41	20.49	6.52	471.38	.00	6.70	.77	7.00	.013	.00	PIPE	
	.0113	-	-	-	-	-	-	.0143	.33	6.89	.77	.013	.00	PIPE	
2447.850	459.970	8.014	467.984	788.41	20.49	6.52	474.50	.00	6.70	.00	7.000	.000	0.0	1 .0	
JUNCT STR	.0083	-	-	-	-	-	-	.0171	.20	8.01	.00	.013	.00	PIPE	
2459.850	460.070	13.269	473.339	461.85	19.44	5.87	479.21	.00	5.32	.00	5.500	.000	0.0	1 .0	
	.0242	-	-	-	-	-	-	.0189	.543	13.27	.00	4.02	.013	.00	PIPE
2747.100	467.030	12.423	479.453	461.85	19.44	5.87	485.32	.00	5.32	.00	5.500	.000	0.0	1 .0	
	.0222	-	-	-	-	-	-	.0189	.804	12.42	.00	4.17	.013	.00	PIPE
3172.300	476.460	11.619	488.079	461.85	19.44	5.87	493.95	.00	5.32	.00	5.500	.000	0.0	1 .0	
	.0226	-	-	-	-	-	-	.0189	.223	11.62	.00	4.06	.013	.00	PIPE
3290.000	479.240	11.359	490.599	461.85	19.44	5.87	496.47	.00	5.32	.00	5.500	.000	0.0	1 .0	
	.0384	-	-	-	-	-	-	.0189	1.82	11.36	.00	3.40	.013	.00	PIPE
3386.260	482.940	9.773	492.713	461.85	19.44	5.87	498.58	.00	5.32	.00	5.500	.000	0.0	1 .0	
JUNCT STR	.0125	-	-	-	-	-	-	.0266	.21	9.77	.00	.013	.00	PIPE	

JTH ESTATES SANDIA MAIN STORM DRAIN  
 TIJERAS ARROYO TO JTH UNIT 1 EXISTING 84" STORM PIPE (FILE:JTH\_F.WSW)  
 STARTING POINT AT MANHOLE 13- ASSUMING JHHUGHES WSEL (2-24-17)

Station	Invert Elev	Depth (FT)	Water Elev	Q (CFS)	Vel (FPS)	Head	Energy Grd. El.	Super Elev	Critical Dia. FT	Flow Top Dia. FT or I.D.	Base Wt Prs/Pip	No Wt Prs/Pip
L/Elem	Ch Slope	-	-	-	-	-	-	-	-	-	-	-
3394.260	483.040	10.856	493.896	364.61	22.93	8.16	502.06	.00	4.45	.00	4.500	.000
37.740	.0670	- -	- -	- -	- -	- -	- -	- -	- -	- -	- -	- -
3432.000	485.570	10.032	495.602	364.61	22.93	8.16	503.76	.00	4.45	.00	4.500	.000
JUNCT STR	.0167	- -	- -	- -	- -	- -	- -	- -	- -	- -	- -	- -
3438.000	485.670	10.742	496.412	357.28	22.46	7.84	504.25	.00	4.44	.00	4.500	.000
248.500	.0384	- -	- -	- -	- -	- -	.0330	8.20	10.74	.00	3.42	.013
3686.500	495.220	10.045	505.265	357.28	22.46	7.84	513.10	.00	4.44	.00	4.500	.000
399.600	.0399	- -	- -	- -	- -	- -	.0330	13.19	10.04	.00	3.37	.013
4086.100	511.150	7.956	519.106	357.28	22.46	7.84	526.94	.00	4.44	.00	4.500	.000
179.300	.0438	- -	- -	- -	- -	- -	.0330	5.92	7.96	.00	3.24	.013
4265.400	519.010	6.535	525.545	357.28	22.46	7.84	533.38	.00	4.44	.00	4.500	.000
JUNCT STR	.0167	- -	- -	- -	- -	- -	.0316	.19	6.54	.00	3.32	.013
4271.400	519.110	7.930	527.040	342.08	21.51	7.18	534.22	.00	4.43	.00	4.500	.000
210.800	.0379	- -	- -	- -	- -	- -	.0303	6.38	7.93	.00	3.32	.013
4482.200	527.090	6.688	533.778	342.08	21.51	7.18	540.96	.00	4.43	.00	4.500	.000
JUNCT STR	.0167	- -	- -	- -	- -	- -	.0270	.16	6.69	.00	3.32	.013
4488.200	527.190	9.809	536.999	303.49	19.08	5.65	542.65	.00	4.39	.00	4.500	.000
98.150	.0470	- -	- -	- -	- -	- -	.0238	2.34	9.81	.00	2.81	.013

## JTH ESTATES SANDIA MAIN STORM DRAIN

TIJERAS ARROYO TO JTH UNIT 1 EXISTING 84" STORM PIPE (FILE:JTH\_F.WSW)  
STARTING POINT AT MANHOLE 13- ASSUMING JHUGHES WSEL (2-24-17)PAGE 6  
Date: 2-27-2018 Time:11: 3:51

Station	Invert Elev	Depth (FT)	Water Elev	Q (CFS)	Vel (FPS)	Head	Grd. El.	Super Elev	Critical Depth	Flow Dia.-FT or I.D.	Top Width	Base Dia.-FT or I.D.	Height ZL	No Wch Prs/Pip	No Wch ZR	Type Ch
L/Elem	Ch Slope	-	-	-	-	-	-	-	-	-	-	-	-	-	-	-
4586.350	531.800	8.379	540.179	303.49	19.08	5.65	545.83	.00	4.39	.00	4.500	.000	.00	1	0	
JUNCT STR	.0167	-	-	-	-	-	.0218	.13	8.38	.00	.013	.00	.00	0	-	
4592.350	531.900	10.321	542.221	276.66	17.40	4.70	546.92	.00	4.35	.00	4.500	.000	.00	1	0	
148.162	.0382	-	-	-	-	-	.0198	2.93	10.32	.00	2.83	.013	.00	0	-	
4740.512	537.561	8.093	545.654	276.66	17.40	4.70	550.35	.00	4.35	.00	4.500	.000	.00	1	0	
HYDRAULIC JUMP	-	-	-	-	-	-	-	-	-	-	-	-	-	-	-	
4740.512	537.561	2.786	540.347	276.66	26.76	11.12	551.46	.00	4.35	.00	4.37	4.500	.000	0	1	
105.188	.0382	-	-	-	-	-	.0403	4.24	2.79	3.07	2.83	.013	.00	0	-	
4845.700	541.580	2.767	544.347	276.66	26.97	11.30	555.65	.00	4.35	4.38	4.500	.000	.00	1	0	
360.400	.0409	-	-	-	-	-	.0387	13.94	2.77	3.11	2.76	.013	.00	0	-	
5206.099	556.330	2.868	559.198	276.66	25.86	10.38	569.58	.00	4.35	4.33	4.500	.000	.00	1	0	
.529	.0405	-	-	-	-	-	.0366	.02	2.87	2.90	2.77	.013	.00	0	-	
5206.628	556.351	2.868	559.220	276.66	25.85	10.38	569.60	.00	4.35	4.33	4.500	.000	.00	1	0	
138.632	.0405	-	-	-	-	-	.0345	4.79	2.87	2.90	2.77	.013	.00	0	-	
5345.260	561.961	2.990	564.951	276.66	24.65	9.44	574.39	.00	4.35	4.25	4.500	.000	.00	1	0	
74.629	.0405	-	-	-	-	-	.0307	2.29	2.99	2.67	2.77	.013	.00	0	-	
5419.889	564.980	3.120	568.100	276.66	23.50	8.58	576.68	.00	4.35	4.15	4.500	.000	.00	1	0	
48.842	.0405	-	-	-	-	-	.0274	1.34	3.12	2.46	2.77	.013	.00	0	-	



